

# Production and mechanical properties of SiC<sub>p</sub> particle-reinforced 2618 aluminum alloy composites

A. Sakthivel · R. Palaninathan · R. Velmurugan ·  
P. Raghothama Rao

Received: 4 June 2007 / Accepted: 30 September 2008 / Published online: 30 October 2008  
© Springer Science+Business Media, LLC 2008

**Abstract** In this study, 2618 aluminum alloy metal matrix composites (MMCs) reinforced with two different sizes and weight fractions of SiC<sub>p</sub> particles upto 10% weight were fabricated by stir cast method and subsequent forging operation. The effects of SiC<sub>p</sub> particle content and size of the particles on the mechanical properties of the composites such as hardness, tensile strength, hot tensile strength (at 120 °C), and impact strength were investigated. The density measurements showed that the samples contained little porosity with increasing weight fraction. Optical microscopic observations of the microstructures revealed uniform distribution of particles and at some locations agglomeration of particles and porosity. The results show that hardness and tensile strength of the composites increased, with decreasing size and increasing weight fraction of the particles. The hardness and tensile strength of the forged composites were higher than those of the cast samples.

## Introduction

The design of Metal Matrix Composite (MMC) is to combine the desirable attributes of metals and ceramics.

The addition of high strength, high modulus refractory particles to a ductile metal matrix produces a material whose mechanical properties are intermediate between the matrix alloy and the ceramic reinforcements. Aluminum metal matrix composites (Al MMCs) are being considered as a group of new advanced materials because of its light weight, high strength, high specific modulus, low co-efficient of thermal expansion, and good wear resistance properties. Combinations of these properties are not available in a conventional material [1–3]. Discontinuously reinforced Al MMCs have not fulfilled their potential for aerospace and automotive applications because of limitations to static performance due to low ductility compared with unreinforced alloys [4–7]. The intrinsic inhomogeneity can give wide scattered value in strength and ductility [6, 7]. The poor tensile ductility compared to the unreinforced counterpart coupled with inferior fracture related properties, size limitations on available product forms, and intrinsic material variability are often severe limitations to the widespread application and use of these composites in performance-critical application [8]. Al MMCs have been used for the automobile products such as engine piston, cylinder liner, brake disk/drum etc., where the wear resistance is very important [9–12].

Processing techniques for Al MMCs can be classified into melt processing (Liquid-phase processing) and powder metallurgy (solid-phase processing) [13]. The powder metallurgy method has better matrix-particle bonding, easier control of matrix structure, and uniform dispersion of the reinforcement [26]. Compared with powder metallurgy, melt processing has some advantages such as simplicity, low cost of processing, manufacturing of intricate components, and near-perfect shape components. Stir casting is generally accepted currently as a commercial practicable method. Its advantages lie in its simplicity,

---

A. Sakthivel · R. Palaninathan  
Department of Applied Mechanics, Indian Institute  
of Technology, Madras, Chennai 600036, Tamilnadu, India

R. Velmurugan (✉)  
Composite Technology Centre, Indian Institute of Technology,  
Madras, Chennai 600036, Tamilnadu, India  
e-mail: ramanv@iitm.ac.in

P. Raghothama Rao  
CEMILAC, DRDO, Bangalore 560 037, India

flexibility, and applicability to large volume production. This melt processing is the most economical of all the available routes for MMC production and allows very large-sized components to be fabricated [14, 15]. However, the melting process has two major problems: First, the ceramic particles are generally not wetted by the liquid metal matrix. Second, the particles tend to sink or float depending on their density relative to the liquid metal and so the dispersion of the ceramic particles are not uniform, whereas powder metallurgy enables uniform distribution of the ceramic particles [26]. In this study, these problems have been overcome by melt stirring at mixing speed and by preheating of the ceramic particles before incorporation into the melt to improve the wettability.

The processing variables such as holding temperature, stirring speed, size of the impeller, and position of the impeller are to be considered in the production of cast MMCs as these variables have impact on mechanical properties [16, 17]. In addition to the above, the other two issues are: (i) wettability; (ii) segregation of the particles. The wettability enhancement methods such as addition of magnesium into matrix, coating or oxidizing the ceramic particles or preheating [16] are available in the literature. Good wetting between the solid ceramic phase and the liquid metal matrix is an essential condition for the generation of a satisfactory bond between these phases. The presence of a gas layer or the formation of an oxide layer on the melt can be detrimental to wettability. In this study, copper coating trial was carried out on silicon carbide particles with electroless copper coating as per procedure laid down in the literature [18]. The coated particles were examined for coating in the Scanning Electron Microscope (SEM) and the result was not encouraging. Hence, preheating was carried out on the particles for the study. The electroless nickel coating would be tried in future.

The fluidity of the composite and settling behavior of the particles during holding as well as during solidification is important. The long holding time may lead to chemical reaction between dispersed particles and the alloy, which will deteriorate the properties of the composites. These aspects have been studied by Rohatgi [19] to conclude that the fluidity of Al-alumina is higher than other composites such as Al-graphite, Al-mica, and Al-SiC<sub>p</sub> due to near-perfect spherical shape of the particles. The decrease in fluidity of Al alloy melts due to the dispersion of ceramic particles can be attributed to the increase in the viscosity of the melts. Extended holding of Al MMC in the liquid state indicates that there is no observable chemical reaction between Al alloy and alumina particles whereas there is little reaction between Al alloy and SiC<sub>p</sub>. The tendency of particle clustering depends on the solidification rate of the melt: lower solidification rate leads to an increase in particle clustering. But particle clustering has no essential

effect on the macroscopic elastic modulus of the composites with different particle distributions as per theoretic prediction using equivalent inclusion method. When subjected to the same macroscopic stress, the clustered region would start yielding at an equal or lower macroscopic stress than that in the unclustered region. The influence of reinforcement clustering on the stress–strain response is not significant of unity aspect ratio, especially in the range of elastic and small plastic strain [20].

Only particulate-reinforced MMC can be formed by the secondary processes such as extrusion, swaging, forging, and rolling. The forming is able to give the reinforcement in a preferential orientation (whiskers for which aspect ratio is greater than one) at which higher mechanical properties can be induced [21]. Similarly, the applied stresses are able to reduce the residual porosity. In order to facilitate matrix flow and to avoid either fracture of the reinforcement or the formation of the voids at the reinforcement–matrix interface, forming is performed at high temperature. Because, the end product is compressor blade, forging is selected as a secondary process. The target properties for making the MMC component are increased strength even at elevated temperature, optimum stiffness, and better fatigue properties. Hence, other processes are not selected for the study. The effect of secondary processes such as extrusion of wrought Al 6061 has been extensively studied [22]. Although, less research has been carried out on forged MMC, there are useful literatures [23, 24] available on 2618 alloys with alumina and SiC<sub>p</sub> particles. Cavaliere et al. [23] discuss about the isothermal forging modeling of 2618 Al alloy reinforced with 20% Alumina particles by employing hot compression tests in the temperature and strain rate ranges of 450–500 °C and 10<sup>-2</sup>–10<sup>-1</sup> S<sup>-1</sup> respectively. In these conditions, the component was isothermally forged with good results in terms of die filling and microstructure. Xu and Palmiere [24] discuss the particulate refinement and redistribution during the axi-symmetric compression of on Al/SiC<sub>p</sub> MMCs. In this study we observed that particulate fracture is more pronounced when specimen was deformed at room temperature, and deformation at elevated temperature results in a more uniform spatial distribution of SiC<sub>p</sub> particles. However, for 2618 (Al–2.3Cu) alloys with SiC<sub>p</sub> particles the literature available is insufficient. Thomas and King [25] have shown that mechanical properties are improved by maintaining optimum solution temperature (546 °C) and time (6 h 33 min) for 2124Al/SiC<sub>p</sub> MMC. Fatigue crack growth rates are reduced by 60% after the optimum solution treatment [25].

Several literatures have highlighted the production methods of MMC for Al alloy with ceramic particles. Most of the literatures are available on Al 2014/SiC<sub>p</sub>, Al 2014/Al<sub>2</sub>O<sub>3p</sub>, and Al 6061/SiC<sub>p</sub> materials with extrusion as a

secondary process for manufacturing. Few articles on powder metallurgy, squeeze casting, and in situ spray process route of manufacturing are available. Most of the articles have projected on the stir casting method. Each author has followed different methods of preparation of specimen for testing. This study differs from earlier investigations in the following ways: (i) a material, namely, 2618 (Al-2.3cu) is used as the matrix, SiC<sub>p</sub> particles are used as a reinforcing material medium, and composite specimens are made by stir casting and (ii) forging as the secondary route. In addition, we have studied on the effects of SiC<sub>p</sub> particles content and size, and the mechanical properties of SiC<sub>p</sub> particle-reinforced 2618 Al alloy composites.

## Experimental work

### Material system

In this study, 2618 Al alloy with the theoretic density of 2760 kg/m<sup>3</sup> is used as the matrix material and SiC<sub>p</sub> (Silicon Carbide) particles of two sizes of 7 and 33 μm and density of 3,200 kg/m<sup>3</sup> are used as the reinforcement. The SiC<sub>p</sub> particles were supplied by Carborundum Universal Ltd. The particle sizes of SiC<sub>p</sub> particles were determined using SEM. The chemical composition of 2618 Al alloy is presented in the Table 1. Six types of test specimens are made, which are classified based on the particle sizes (7 and 33 μm) and wt.%(0, 5, and 10). The particle size is nearly uniform of either 7 or 33 μm.

### Specimen preparation

Experimental set-up was made for making the MMC casting blanks. The Silicon-type heater with 2-KW power rating and maximum temperature capacity of 1,000 °C, was used. The temperature was measured by K-type thermocouple with the solid-state relay temperature controller with the temperature accuracy of ±1 °C. The melting process was carried out in a graphite crucible with upper diameter 110 mm and lower diameter 95 mm. The mixing was carried out by turbine-type stirrer with variable universal motor of portable hand-drilling machine. It has the speed range of 600–2,400 rpm. The turbine rotor has four blades with 90° angle to each blade. The experimental set up is shown in Fig. 1.

**Table 1** Chemical composition of 2618 Al alloy matrix (wt.%)

Si	Mn	Cu	Fe	Mg	Ni	Ti	Ti-Zr	Zn	Al
0.2	0.2	2.3	1.1	1.5	1.1	0.2	0.25	0.15	Balance

Initially, 2618 Al alloy was charged into the crucible and heated to about 750 °C till the entire alloy in the crucible was melted [11]. The ceramic particles were preheated to 900 °C [9, 10] for 1 h before incorporation into the melt. The steel mold of size 150 × 120 × 30 mm<sup>3</sup> was used for the preparation of cast blanks. The mold was also preheated to 550 °C [26] for 10 min to obtain uniform solidification. After the molten metal was fully melted degassing tablet was added to reduce the porosity. The stirrer was lowered into the melt slowly to stir the molten metal at the speed of 700 rpm [2, 11]. The preheated SiC<sub>p</sub> particles were added at the rate of 40 g/min during the stirring time. The stirring was continued for another 5 min even after the completion of particle feeding. The temperature was also monitored simultaneously during stirring when the temperature remained between 700 and 720 °C [3, 11]. The mixture was poured into the mold. The maximum duration of mixing was 10 min. The clearance of the stirrer from the bottom of the crucible was approximately 10 mm with the melt depth of 100 mm.

The cast blanks were milled to the perfect shape to remove the remnant particles or cold shuts. The cast MMC samples were forged to break the cast structure to get uniform grain/equiaxial grains for the improvement of properties to the level of extruded bar. The minimum requirement for the forgings with the reduction ratio is four. The forging operation was carried out with the hammer capacity of 500 kg m. For each operation, temperature of 450 °C was maintained for the duration of 2 h. Three such operations were carried out in three directions. When the third operation was carried out, samples tend to crack at the surface. The forged MMCs were then subjected to heat treatment cycle mentioned below:

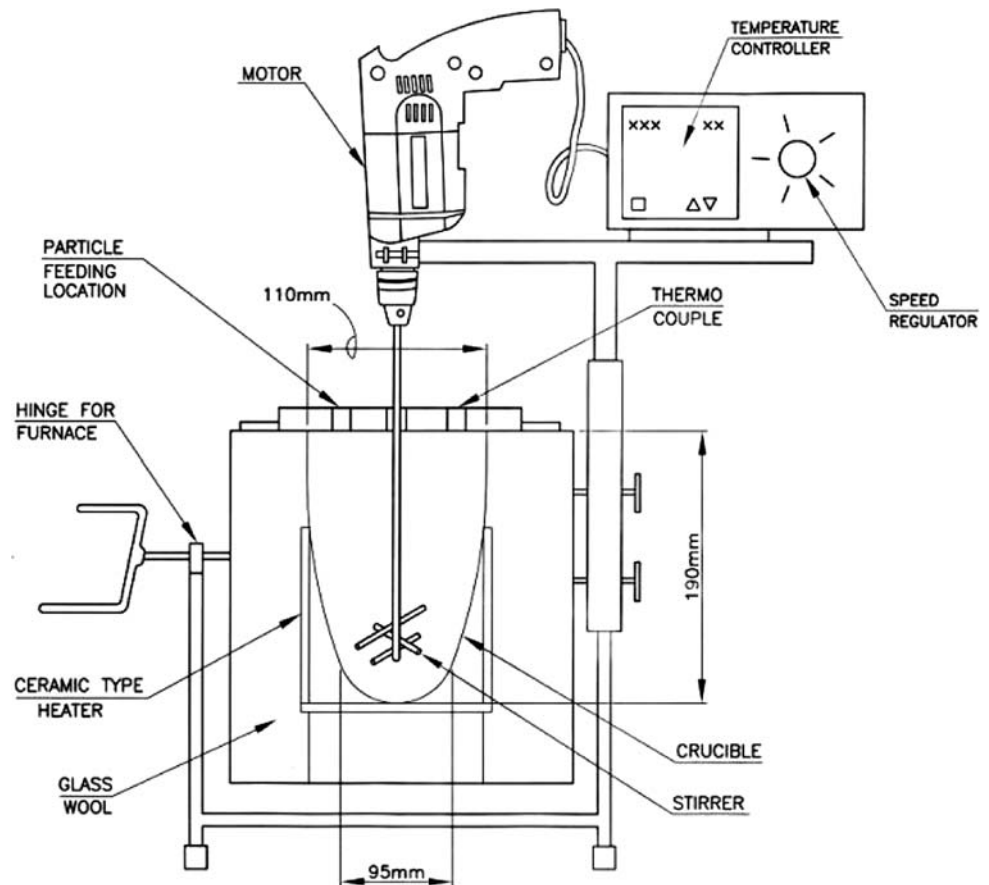
- Maintained 525 °C for 2 h followed by water quenching
- Precipitate hardening at 175 °C for 10 h

It was observed that MMCs behave differently in different directions while forging compared to the unreinforced material.

### Microstructure characterization

Metallographic samples cut from the cast and forge billet, mounted on bakelite with wet ground between 400 and 600 grit SiC<sub>p</sub>-impregnated emery surface using copious amounts of water as lubricant. The polishing operation was carried out on Mecapol P230 programmable polishing machine with the speed range from 20 to 600 rpm. Fine polishing to near mirror-like finish was achieved using lavigated alumina powder suspended in distilled water. Reinforcement morphology and its distribution in the MMC along with other intrinsic microstructural features

**Fig. 1** Experimental set up for casting



were identified by examining the samples in an optical microscope (Nikon EPIPHOT-TME inverted Microscope) with metal power image analyzer.

### Testing

The experimental density of the composites was obtained by the Archimedeian method of weighing small pieces cut from the composite billet, first in air and then in water. The porosities of the produced composites can be evaluated from the difference between the expected and the observed density of each sample. Six specimens for each percent weight fraction of  $\text{SiC}_p$  were used for density measurement.

Hardness of the MMC samples was measured in the EMCO hardness tester after polishing to 1  $\mu\text{m}$  finish. The brinell hardness values of the samples were measured using a ball diameter of 1 mm with 10 kg load to obtain an indentation which would be representative of the macro-structure of the material. In order to eliminate the possible segregation effects, the mean of the six tests was carried out for each specimen.

The specimens were machined to the specification outlined in ASTM E8, ASTM E21 and ASTM E-23. The

length to diameter ratio of the mechanical test specimen was chosen, so as to minimize buckling during fully reversed (Tension-compression) stress amplitude-controlled cyclic deformation. To minimize the effect of surface irregularities, the test specimen surface was prepared by mechanically polishing the gauge section using progressively finer grade of silicon carbide-impregnated emery paper and then finish polished using 0.5  $\mu\text{m}$  alumina powder suspended in distilled water so as to obtain a mirror-like finish that is free of all circumferential scratches and surface machining marks.

The tensile and hot tensile tests were performed on a TIRA 2820S universal material testing machine with a modular test system. The testing machine suitable for examining the strength and deformation behavior of solid materials during tensile, compression and bending tests upto 20 KN. For the measurement of force, strain gauge load cells are provided with the measuring cycle less than 22 ms. It has the capability of operating in the speed range of 0.01–1,000 mm/min. The tests were conducted in controlled laboratory air environment at ambient temperature (27 °C). Tensile tests were conducted in accordance with procedures outlined in ASTM E8 at a strain rate of 2 mm/min. The strain was measured with the LVDT.

Hot tensile tests were conducted in the same machine in accordance with procedures outlined in ASTM E21 at a strain rate of 2 mm/min. The maximum temperature capability to perform hot tensile test is 1,100 °C. The de-rated temperature chosen was 120 °C, which corresponds to the maximum temperature of the end product application.

Izod impact test was carried out on single notch cylindrical specimens as per procedure outlined in ASTM E23.

### Results and discussions

#### Production of composites

In this study, 2618 Al alloy reinforced with different particle sizes (7 and 33 μm) and weight fractions (5 and 10wt.%) of SiC<sub>p</sub> particles have been produced using stir cast method and subsequent forging. Various trials have been carried out before making MMC samples. Figure 2 shows the different types of stirrers used in the trials, but turbine-type stirrer has provided good mixing [27–29] because the development of the vortex during stirring is helpful for transferring the particles into the matrix melt as the pressure difference between the inner and the outer surface of the melt sucks the particles into the liquid with the limited stirrer speed. In the present study, Zig Zag and Graft types of stirrers were used. Zig Zag type of stirrer experienced with vigorous mixing and spilling over the crucible. Graft (Helical ribbon) type of stirrer has not created any vortex and settled without mixing. It was confirmed by subsequent metallographic assessment of the casting.

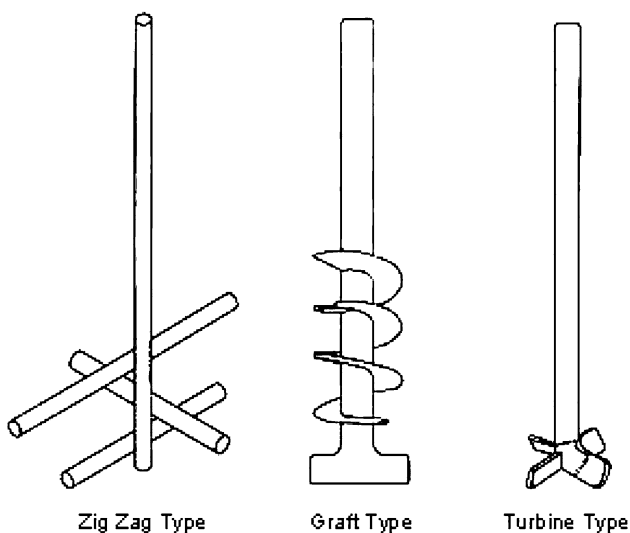


Fig. 2 Types of stirrer

The experiment was conducted for the Stirrer speeds of range from 700 to 1,000 rpm based on the literature [26]. In this study, it is observed that the distribution of the particle in the micrograph is uniform at 700 rpm [26] and hence stirrer speed was selected as 700 rpm. The position of the Impeller at 1/10 of the melt depth from the bottom of the crucibles is fixed as per literature [26]. Particularly at higher rpm, vortex is formed on the surface of the molten metal [30]. Figure 3 shows the cast billet manufactured by the above process conditions and Fig. 4 shows the cracked surface of the billet after forging.

#### Microstructure

Figure 5a and b is the optical micrograph of Al alloy and Fig. 5c and d is the optical micrograph of Al alloy with 10wt.% SiC<sub>p</sub> particles (7 μm) composite. An uniform dispersion of the particles is achieved as shown in the figure. In composites, the SiC<sub>p</sub> particles are of non-uniform size in



Fig. 3 Cast billet

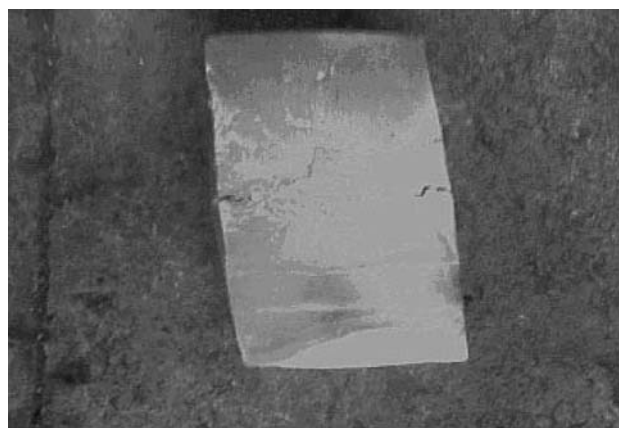
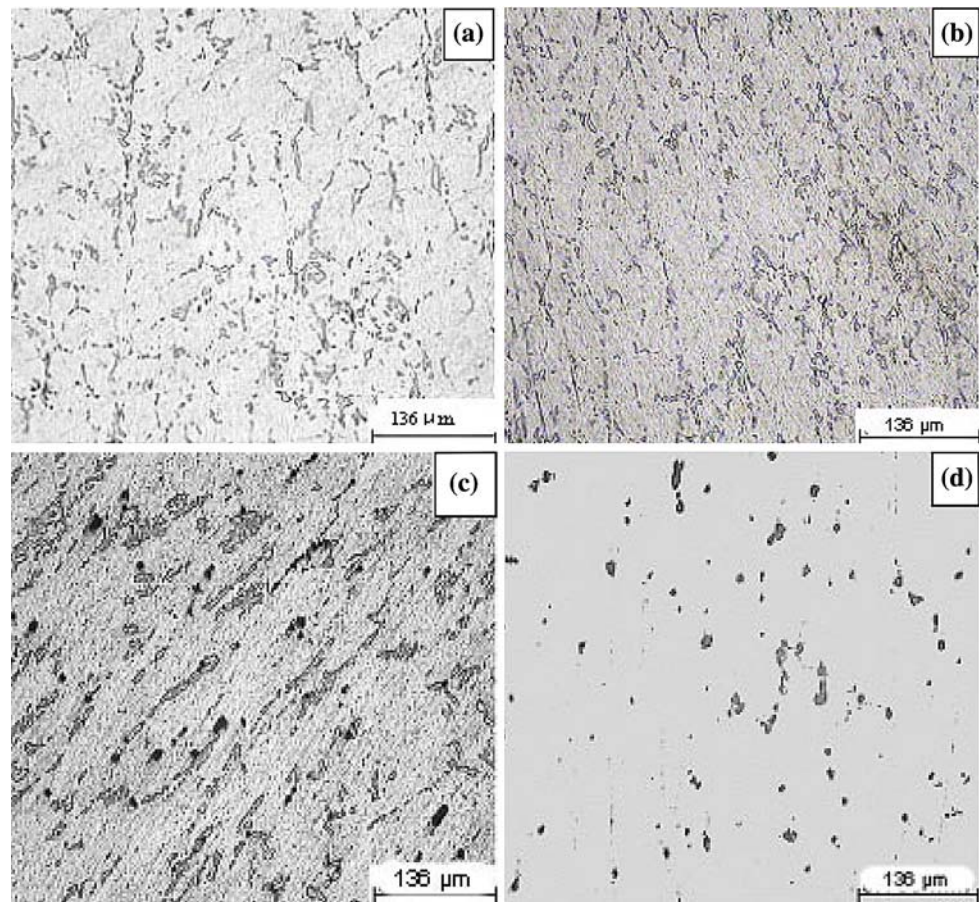


Fig. 4 Cracked surface of the forged billet

**Fig. 5** **a** and **b** is the optical micrograph of Al alloy. **c** and **d** is the optical micrograph of Al alloy reinforced with 10wt.% SiC<sub>p</sub> particles (7 μm size) and stirrer rpm: 700, black regions are SiC<sub>p</sub> particles



the range of 5–10 μm. Figure 6a and b is the optical micrograph of Al alloy reinforced with 5 and 10wt.% SiC<sub>p</sub> particles (7 μm) composites respectively. Figure 6c and d is the optical micrograph of Al alloy reinforced with 10wt.% SiC<sub>p</sub> particles which shows porosity and particle segregation. In order to confirm the presence of SiC<sub>p</sub> particles, Energy dispersive X-ray analysis (EDX) was carried out in the SEM. Figure 7a and b indicates SEM micrographs of composite reinforced with 10wt.% SiC<sub>p</sub> particles which shows agglomeration. Agglomeration or clustering of the particles was also observed, resulting in particle-rich regions. Figure 7c shows the EDX spectrum with silicon and carbon indications. The agglomeration site consists of the larger SiC<sub>p</sub> particles intermingled with smaller and regularly shaped SiC<sub>p</sub> particles. The reason for the segregation and agglomeration of the particles and porosity is as follows: The Al dendrites solidify first during solidification of the composites, and the particles are rejected by the solid–liquid interface and hence segregated to the interdendrite region.

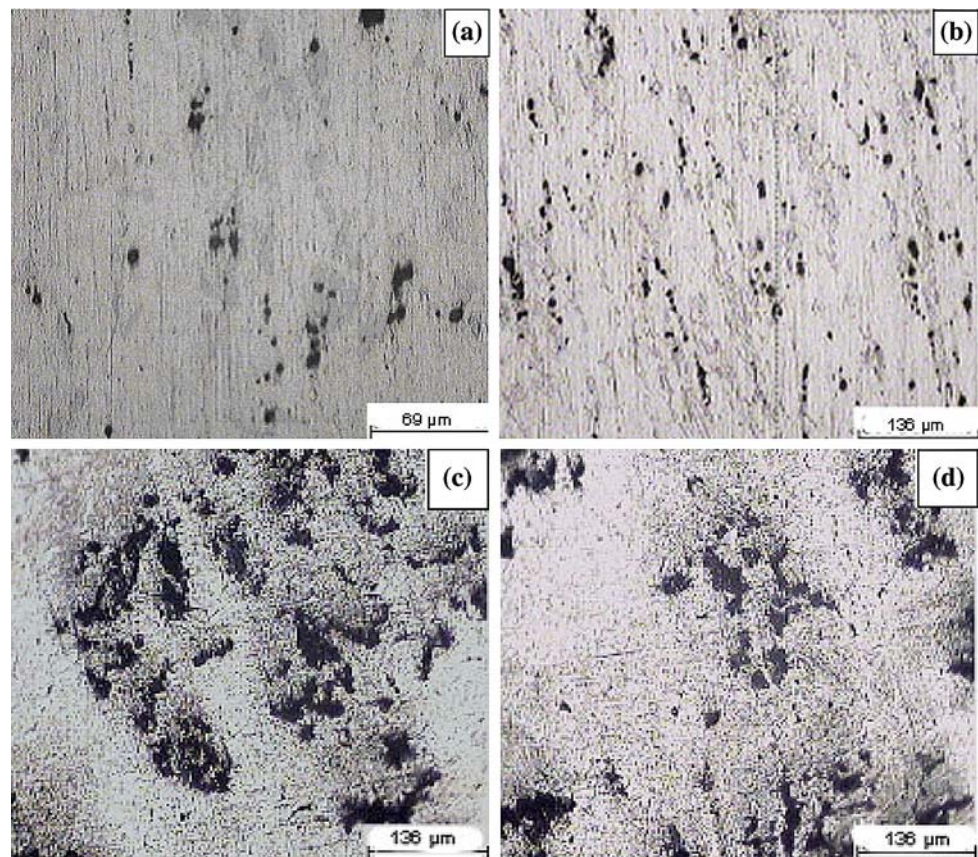
Figure 6c and d is the optical micrograph of Al alloy with SiC<sub>p</sub> particles (7 μm) composite for the stirrer speed of 1,000 rpm. The speed of rotation of the stirrer is seen to

have significant impact on fluid flow characteristics of both velocity of flow and direction.

#### Test results

The experimental densities of the composites according to the weight fractions of the SiC<sub>p</sub> particles are shown in Fig. 8. Figure 8 shows that the theoretic density values of the composites increase linearly (as per the rule of mixtures). The experimental densities are lower than that of the theoretic densities. The values of density in composites increase with increasing weight fraction and size of the particles. Density of SiC<sub>p</sub> is higher than the Al alloy and hence the increase in wt.% of SiC<sub>p</sub> will increase the density of the composite based on the rule of mixtures. During the production process of the MMCs, some porosity level is normal, because of the long particle feeding and the increase in surface area in contact with air. The forging operation will reduce the porosity level of the casting. The porosity for 33 micron particles at 5wt.% fraction is 0.32% and for 10wt.% fraction it is 0.64%. The corresponding values for 7 micron particles are 0.36% and 0.75% for 5% and 10wt.% fractions respectively. The porosity of the

**Fig. 6** **a** and **b** is the Optical Micrograph of Al alloy reinforced with 5 and 10wt.% SiC<sub>p</sub> particles (7 μm size) and stirrer rpm: 700, black regions are SiC<sub>p</sub> particles. **c** and **d** is the optical micrograph of Al alloy reinforced with 10wt.% SiC<sub>p</sub> particles with porosity and particle segregation, stirrer rpm: 1000



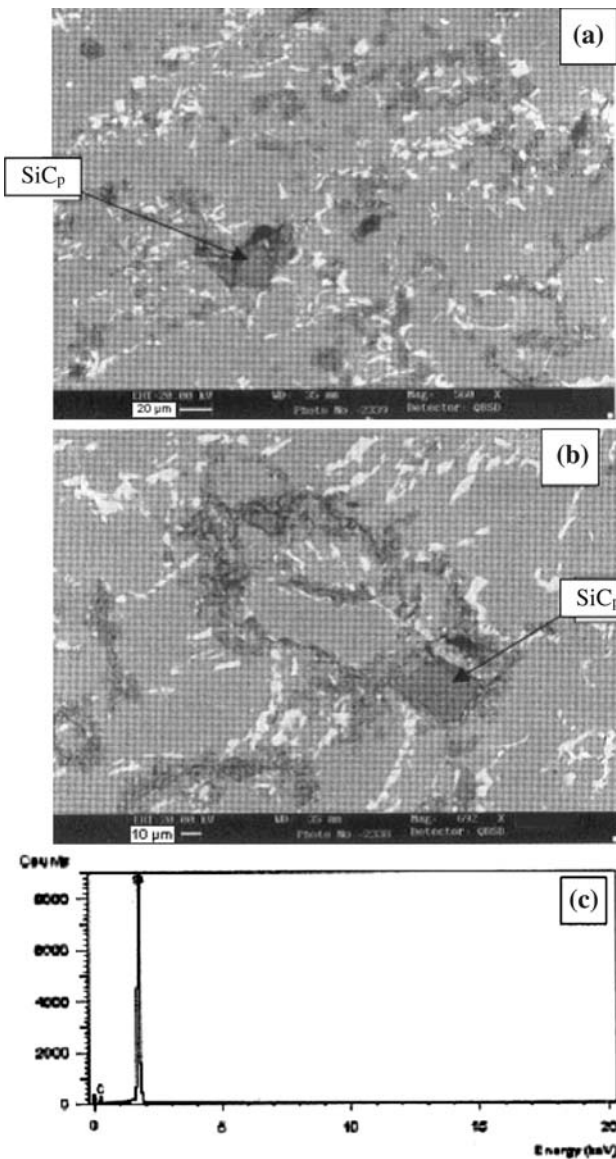
composites increases with the increasing wt.% of the particle. Similar observations have also been made in [26]. It is understood that the amount of porosity is less for forge component than cast. This is because of application of pressure during forging operation.

Hardness tests were performed on a Brinell hardness machine and the results of the tests for the cast and forge specimens with different particle sizes are shown in Fig. 9. From the figure it is observed that hardness increases with the amount of SiC<sub>p</sub> particles and decreases with increase of particle size. The hardness of the forge specimens has increased by 5–7% from the cast specimens. The percent increase in hardness is reduced with increase of wt.% of particle. Since SiC<sub>p</sub> is hard, the addition of the same with Al alloy can increase the hardness with increase in SiC<sub>p</sub> wt [26]. The density and hardness are decreasing with particle size. The percent increase in hardness is reduced with increase of wt.% of particle. With the increase in percent weight of SiC<sub>p</sub> particle in the beginning [5wt.%], it makes the MMC harder because of SiC<sub>p</sub>'s brittle nature. Subsequent addition of particle increases the hardness at low rate since, earlier addition itself is closer to the maximum level.

The results of the tensile tests at room temperature and hot tensile test (at 120 °C) are shown in Figs. 10, 11, 12,

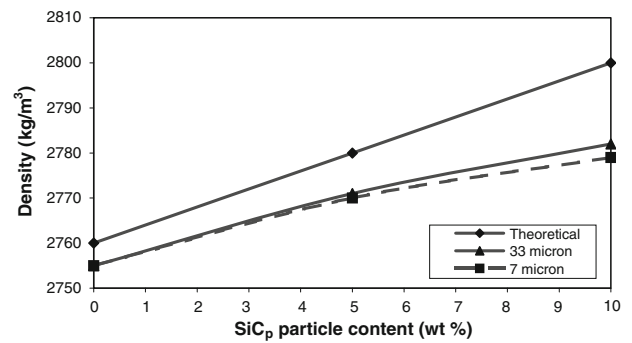
and 13 with the wt.% fraction for different sizes of SiC<sub>p</sub> particles. Figure 10 indicates the variation of tensile strength with the percent weight fraction and size of SiC<sub>p</sub> at room temperature. From the figure, the ultimate tensile strength (UTS) and 0.2% proof strength (PS) increase with increase in percent weight fraction and decrease with particle size. Figure 11 shows the variation of elongation with SiC<sub>p</sub> particle content and size at room temperature. The elongation measured for the composites drastically reduced to more than 50% and then becomes almost constant with further increase in percent weight fraction. Figure 12 indicates the variation of tensile strength with the percent weight fraction at 120 °C. In the hot tensile test (at 120 °C) also UTS and 0.2% PS increase with increase in percent weight fraction and decrease with particle size. But tensile strength is less at 120 °C than room at temperature.

Figure 13 represents the variation of elongation with the percent weight fraction of SiC<sub>p</sub> particle content and size at 120 °C. However, the elongation of composites at 120 °C is marginally higher than that at room temperature. The elongation decreases with decrease of particle sizes. Most of the MMCs are less ductile at room temperature and ductility will increase at elevated temperature because of climb/gliding mechanisms. The elongation measured for the composite lies with a very low range depending on the



**Fig. 7** **a** is the SEM micrographs of composite reinforced with 10wt.% SiC<sub>p</sub> particles (7 μm size) and stirrer rpm: 700. **b** is the SEM micrographs of composite reinforced with 10wt.% SiC<sub>p</sub> particles with agglomeration (7 μm size) and stirrer rpm: 1000. **c** is the EDX spectrum with silicon and carbon indications

SiC<sub>p</sub> particle size and content. Higher the particle content, lower the elongation due to the increase in UTS and 0.2% PS. This means that the ductility is controlled and brittleness is increased. Figure 14 indicates the results of the Izod impact test at room temperature. As shown in the figure, the impact energy value decreases with increase in percent weight fraction and increase with increasing particle size. Similar trend is also observed in [31]. The lower impact strength of MMCs can be attributed to the presence of brittle SiC<sub>p</sub> particles, which may act as stress concentration zone. Further, the heterogeneous dispersion of SiC<sub>p</sub> particles in the matrix resulting in the formation of clusters has



**Fig. 8** Variation of theoretic and experimental densities with SiC<sub>p</sub> particle content and size

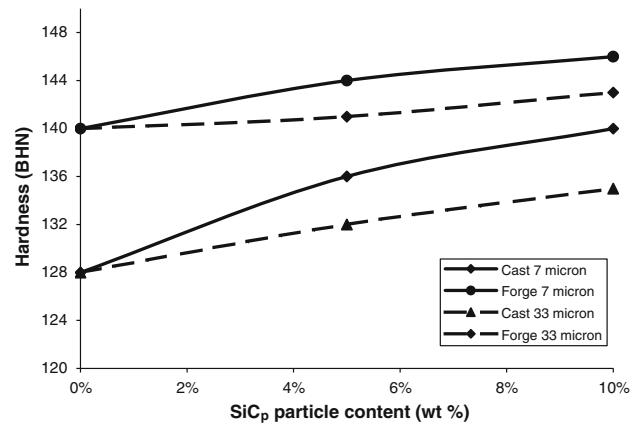


**Fig. 9** Variation of hardness with SiC<sub>p</sub> particle content and size

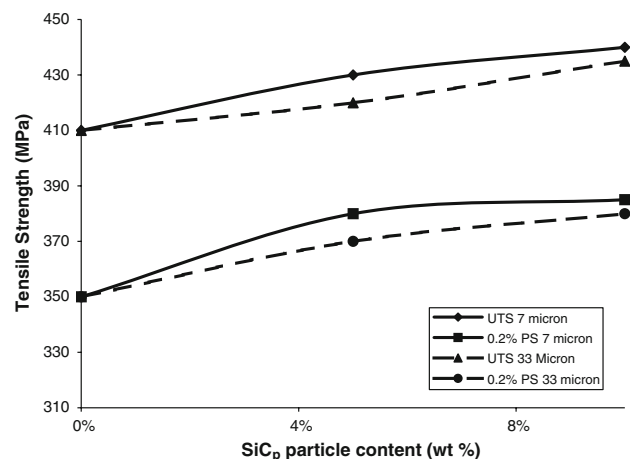


**Fig. 10** Variation of tensile strength at room temperature with SiC<sub>p</sub> particle content and size

reduced the matrix reinforced bonding and the impact energy.

Among all of the MMCs, the composites reinforced with 7 μm SiC<sub>p</sub> particles have the maximum hardness and tensile strength and the minimum elongation. Reinforcements have led to the strengthening of the non-uniform strain



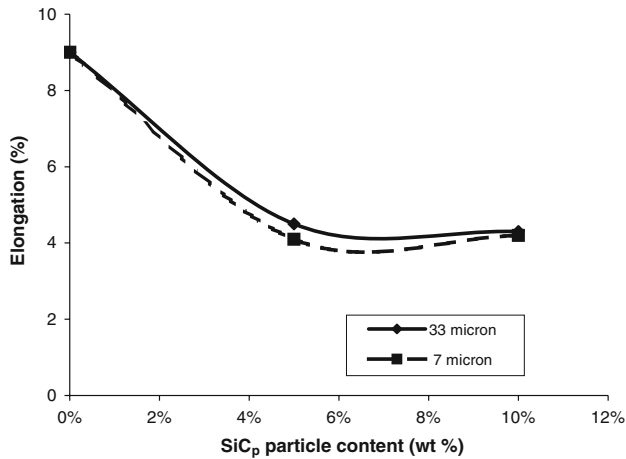


**Fig. 11** Variation of elongation at room temperature with SiC<sub>p</sub> particle content and size

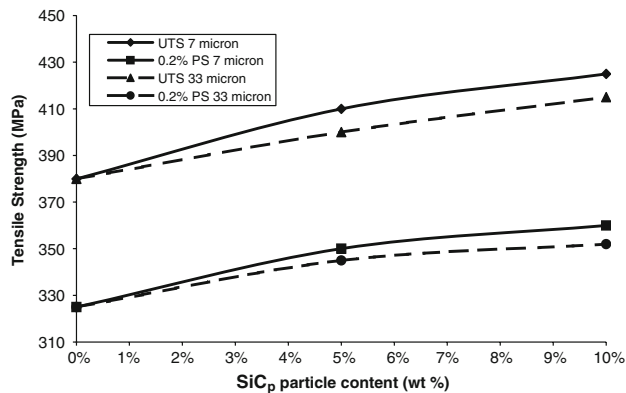


**Fig. 12** Variation of tensile strength at 120 °C with SiC<sub>p</sub> particle content and size

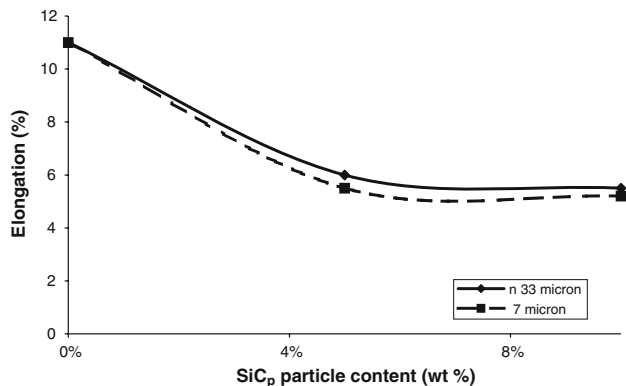


**Fig. 13** Variation of elongation at 120 °C with SiC<sub>p</sub> particle content and size

distribution. Strain in the local region is sufficiently high and the matrix fails in tension at lower strain than the unreinforced matrix. This leads to a decrease in tensile ductility than the unreinforced matrix. We concluded from

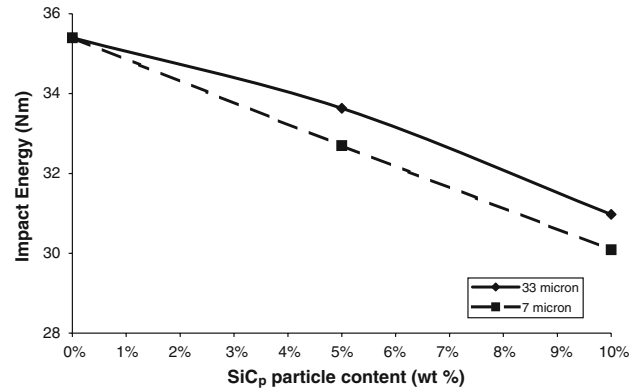


**Fig. 14** Variation of impact energy with SiC<sub>p</sub> particle content and size

the studies that the addition of ceramic particles can increase the strength and hardness based on the concept of rule of mixtures. The reduction in fracture toughness and ductility is due to the addition of brittle nature of ceramic particle to ductile matrix material, which leads to low ductility type of MMC. The stir casting method is limited up to 10% weight fraction of ceramic particles. In future, use of semi-solid stage mixing and application of pressure after casting in place of forging for better wettability to avoid the crack will be studied. Based on the findings of the investigation, properties such as tensile strength and ductility are within the intended application. However, fatigue properties are yet to be established to fulfill the required properties.

### Conclusions

The optimum process conditions were found in this study for production of SiC<sub>p</sub> particle-reinforced Al alloy composites by the stir casting method followed by forging. Optical micrograph, density, tensile strength and elongation at room temperature and at 120 °C, and impact strength of MMCs were investigated. The following conclusions have been drawn:

- (1) Optical micrograph indicates the uniform distribution of SiC<sub>p</sub> particles with clustering at few locations.
- (2) The density of the composites increased with increasing weight percentage and size of particles.
- (3) The hardness of the composites increased with increasing weight percentage and decreasing size of particles.
- (4) UTS and 0.2% PS increases with increase in weight percentage at room temperature and higher temperature (120 °C) conditions. The percent elongation is decreased nearly 50% for Al MMC when compared with unreinforced Al alloy.

- (5) Impact strength of the composites decreased with increasing weight percentage and decreased with decreasing size of particles.

**Acknowledgement** The authors wish to express gratitude to HAL (Hindustan Aeronautics Limited), Bangalore, India for providing the facilities to carry out experiments, pertaining to this study.

## References

1. Surappa MK, Rohatgi RK (1981) *J Mater Sci* 16:983
2. Hanumanth GS, Iron GA (1993) *J Mater Sci* 28:2459
3. Sahin Y, Murphy S (2014) *J Mater Sci* 34(1996):5399
4. Papazian JM, Adler PN (1990) *Metall Trans* 21A:401
5. Carcalho MH, Marcelo T, Carvalhinos H, Cellars CM (1992) *J Mater Sci* 27:2101
6. Ceschini L, Minak G, Morri A (2006) *Compos Sci Technol* 66:333
7. Shorowordi KM, Laoui T, Hasseb ASMA, Celis JP, Froyen L (2003) *J Mater Process Technol* 142:738
8. Srivatsan TS, Al-Hajri M (2002) *Compos Part B* 33:391
9. Gibson PR, Clegg AJ, Das AA (1985) *Mater Sci Technol* 1:558
10. Dellis MA, Keastemans JP, Dellanay F (1991) *Mater Sci Eng* 135A:253
11. Rohatgi PK (1991) *J Metals* 43(4):10
12. Kocazac MJ, Khatri SC, Allison JE, Bader MG et al (1993) In: Suresh S et al (eds) *Fundamentals of metal matrix composites*, Butterworths, Guildford, UK, p 267
13. Srivatsan TS, Ibrahim IA, Mohamed FA, Lavernia EJ (1991) *J Mater Sci* 26:5965
14. Sahin Y, Kok M, Celik H (2002) *J Mater Process Technol* 128:280
15. Taha MA, El-Mahallawy NA (1998) *J Mater Process Technol* 73:139
16. Delannay F, Froyan L, Deruyttere A (1987) *J Mater Sci* 22:1
17. Seo YH, Kang CG (1985) *J Mater Process Technol* 55:370
18. Davidson AM, Regener D (2000) *Compos Sci Technol* 60:865
19. Rohatgi PK, Sathyamoorthy R, Narendranath CS, Nath D (1993) *AFS Trans* 101:597
20. Tszeng TC (1998) *Compos: Part B* 29B:299
21. Girot FA, Quenisset JM, Naslain R (1987) *Compos Sci Technol* 30:155
22. Lianxi H, Shoujing L, Wencan H, Wang ZR (1995) *J Mater Process Technol* 49:287
23. Cavaliere P, Cerri E, Evangelista E (2004) *J Alloy Compd* 378(1–2):117
24. Xu H, Palmiere EJ (1999) *Compos Part A* 30:203
25. Thomas MP, King JE (1996) *Compos Sci Technol* 56:1141
26. Kok M (2005) *J Mater Process Technol* 161:381
27. Harnby N, Edward MF, Nienow AW (1985) *Mixing in process industries*. Butterworths, London
28. Hashim J, Looney L, Hashmi MSJ (1999) *J Mater Process Technol* 92–93:1
29. Naher S, Brabazon D, Looney L (2003) *J Mater Process Technol* 143–144:567
30. Hashim J, Looney L, Hashmi MSJ (2002) *J Mater Process Technol* 123:258
31. Ozden S, Ekici R, Nair F (2007) *Compos Part A* 38(2):484